Ultrasonics - Sonochemistry 52 (2019) 184–192

Contents lists available at ScienceDirect

Ultrasonics - Sonochemistry

journal homepage: www.elsevier.com/locate/ultson

Preparation of low molecular weight heparin using an ultrasound-assisted Fenton-system

Zijian Zhi[a], Junhui Li[a], Jianle Chen[a,b], Shan Li[a], Huan Cheng[a], Donghong Liu[a], Xingqian Ye[a], Robert J. Linhardt[b,*], Shiguo Chen[a,*]

[a] Zhejiang Key Laboratory for Agro-Food Processing, Department of Food Science and Nutrition, Fuli Institute of Food Science, Zhejiang University, Hangzhou 310058, China

[b] Center for Biotechnology & Interdisciplinary Studies, Department of Chemistry & Chemical Biology, Rensselaer Polytechnic Institute, Biotechnology Center 4005, Troy, NY 12180, USA

ARTICLE INFO

Keywords:
Heparin
Depolymerization
Sono-Fenton
Anticoagulant activity

ABSTRACT

Heparin, a high-molecular weight acidic polysaccharide, has raised much interest in the field of biomedical research due to its multiple bio-functions. The anticoagulant application of heparin in routine clinical practice, however, has been limited as the large molecular size of heparin can reduce its subcutaneous bioavailability and lead to severe adverse consequences such as thrombocytopenia. Here, we report a highly efficient and convenient method to depolymerize high-molecular weight, unfractionated heparin (UFH), into low molecular weight heparin (LMWH) by combining physical ultrasonic treatment with the chemical Fenton reaction, referred to as sono-Fenton. We found that this combination treatment synergistically degraded UFH into a LMWH of 4.87 kDa within 20 min. We characterized the mechanism of sono-Fenton heparin degradation through multiple approaches, including HPLC-SAX, disaccharide composition, FT-IR, NMR and top-down analysis, and found that the uronic acid residue in heparin was the most susceptible site attacked by ·OH radicals produced in the sono-Fenton process. Importantly, the LMWH prepared by this method had significantly higher anticoagulant activity than UFH and other LMWHs. This approach represents an effective method to produce heparin with improved activity and should be potentially useful for heparin production in the pharmaceutical industry.

1. Introduction

Heparin was discovered in liver tissue by Jay McLean in 1916 and officially applied as an anticoagulant in clinical medicine by 1937 [1]. It is a highly sulfated glycosaminoglycan with a complex structure, composed of repeating disaccharide units of *N*-acetylated or *N*-sulfated D-glucosamine that are α-(1-4)- or β-(1-4)-linked to L-iduronic or D-glucuronic acids [2]. The special pentasaccharide sequence in heparin has a high affinity for binding to antithrombin III (AT) and activates it, indicating that the affinity of heparin for AT is the basis for heparin's anticoagulant effect [3]. However, UFH, which has an average molecular weight (Mw) of ~15 kDa [4], can cause heparin-induced thrombocytopenia (HIT) due to the binding of heparin to platelet factor 4 (PF4), forming an antigenic complex that stimulates the body to produce antibodies. In addition, UFH shows a risk of bleeding in clinic practice, which limits its long-term clinical application [5]. Hence, LMWH, whose Mw is approximately 5 kDa, has emerged the heparin of choice for many clinical applications. LMWH shows a greatly reduced binding to proteins that decreases its immunogenicity.

Commercial LMWHs have been prepared by physical separation, chemical depolymerization and enzymatic modification [6]. Although LMWHs can be recovered by physical separation from UFH, the target product yield is low and this results in a serious waste of raw materials. Chemical modifications, such as nitrous acid cleavage and chemical ß-elimination, have been widely used in heparin industry. However, chemical waste and contamination are major problems of these chemical processes and the required degradation time is generally more than 4 h. Enzymatic depolymerization offers many advantages, such as the mild reaction conditions, high selectivity and low environmental adverse effects, but the limited availability of specific enzymes and their high costs tend to limit their broad industrial application.

Ultrasound treatment has been regarded as an effective and green technique without introducing secondary pollutants during the processing [7]. The use of ultrasound offers a promising means to depolymerize a variety of polysaccharides. Ultrasound can produce the acoustic cavitation that involves the formation, collision and

* Corresponding authors.
E-mail addresses: linhar@rpi.edu (R.J. Linhardt), chenshiguo210@163.com (S. Chen).

https://doi.org/10.1016/j.ultsonch.2018.11.016
Received 8 August 2018; Received in revised form 13 November 2018; Accepted 19 November 2018
Available online 20 November 2018
1350-4177/

subsequent expansion of micro-bubbles during sonication, generating hydroxyl radicals that break polysaccharides [8]. Polymers would not be completely degraded by ultrasound because of the attenuation of energy transmission under a prolonged or high-intensity ultrasonic field. Hence, there have been some attempts to combine ultrasound with the use of chemicals [9] and enzymes [10] to improve its degradation efficiency.

The Fenton system, one of the most promising advanced oxidation reactions, utilizes ferrous ion as the catalyst to enhance the production of OH· radicals from hydrogen peroxide (Eq. (1)). The Fenton system involves a complicated array of reactions and is controlled by Fenton reagent concentration, reaction temperature and pH. Fenton chemistry assisted by ultrasound can actually increase degradation efficiency [11]. However, there are no reports using Fenton chemistry combined with ultrasound to prepare LMWHs.

$$Fe^{2+} + H_2O_2 \rightarrow Fe^{3+} + HO\cdot + OH^- \quad (1)$$

In the present work, we combined Fenton chemistry with ultrasound to prepare LMWHs with suitable Mw and optimized reaction conditions to obtain efficient degradation. Disaccharide compositional analysis, Fourier transform infrared spectroscopy (FT-IR), nuclear magnetic resonance (NMR) spectroscopy and top–down analysis were performed to understand the heparin degradation mechanism of the sono-Fenton system. The anticoagulant activities of LMWHs prepared were also determined.

2. Materials and methods

2.1. Chemicals and materials reagents

Dextran was purchased from Sigma Chemical Co. (St. Louis, MO, USA). Heparin, hydrogen peroxide, ferrous chloride tetrahydrate, hydrochloric acid, HPLC-grade methyl alcohol and deuterium oxide were obtained Sinopharm Chemical Reagent Co., Ltd. (Shanghai, China). APTT assay reagent, TT assay reagent and calcium chloride (0.025 M) were from Nanjing Jiancheng Bioengineering Institute (Nanjing, China).

2.2. Electron spin-resonance (ESR) spectra of different reaction processes

OH· radicals were trapped by dimethyl sulfoxide and investigated using an ESR spectrometer. ESR spectra were obtained in X-band at room temperature and the spin adduct was quantified. The operating parameters were as follows: the sweep width, 100 G, sweep time, 1 min, time constant, 0.1 s, microwave power, 0.998 mW, modulation frequency, 100 kHz, modulation amplitude, 20 G.

2.3. Fenton system combined with ultrasound for degradation of heparin

Ultrasound treatments (Scientz-IID, Ningbo Scientz Biotechnology Co., Ningbo, China) were carried out with the following parameters: frequency, 22 kHz, maximum ultrasonic output power, 900 W, intermittent type, 2 s on and 2 s off, ultrasonic probe diameter, 10 mm. We put 25 mL heparin solution (5 mg/mL) into a cylindrical glass reactor (Φ, 2.9 cm) and positioned the ultrasonic probe below the liquid surface of 1 cm for release of energy.

2.3.1. Optimization of the parameters of sono-Fenton process

The effects of the following factors were surveyed: temperature (10, 20, 30 and 40 °C), ultrasonic intensity (0, 3.8, 7.6, 11.4 and 15.2 W/mL), hydrogen peroxide (30 wt%) at various concentrations (2, 4, 6, 8, 10 g/L), ferrous concentration (0.5, 1.0, 1.5 and 2 mM) and pH (3, 4, 5, 6, 7) (Table 1). The general degradation parameters of all the tests were as follow: duration time of 60 min, temperature at 30 °C, ultrasonic intensity of 3.8 W/mL, ferrous concentration of 1.5 mM, hydrogen peroxide dose of 6 g/L and pH at 3. The reaction was stopped by adding excess sodium bisulfite. Fe^{2+} and Fe^{3+} could be completely removed by passing the reaction mixture through cation-exchange resin. The LMWHs could be recovered through alcohol precipitation, which was followed by freeze-drying for later use.

Table 1
Single-factor experimental design of heparin degradation.

Item	Parameters	Range
Sono-Fenton process	Temperature (°C)	10, 20, 30, 40
	Ultrasonic intensity (W/mL)	0, 3.8, 7.6, 11.4, 15.2
	Hydrogen peroxide (g/L)	2, 4, 6, 8, 10
	Fe^{2+} concentration (mM)	0.5, 1.0, 1.5, 2.0
	pH	3, 4, 5, 6, 7

2.4. Determination of the Mw of UFH and LMWHs

The Mw was detected by a high performance size exclusion chromatography (HPSEC) as described previously [12] with some modifications. Sample solution (40 μL) was injected into Waters 1525 HPLC system (Waters, Milford, USA) and eluted by sodium chloride solution (0.2 M) at 40 °C for 30 min at a flow rate of 0.5 mL/min. The eluent was monitored with a Waters 2414 refractive index detector (Waters, Milford, USA). Standard dextrans (1.27, 5.22, 11.60, 2.38 and 5.22 kDa) were used to acquire a calibration curve. The Mw of heparin samples was calculated using this calibration curve with Breeze 2 software.

2.5. Determination of disaccharide composition

Disaccharide analysis was performed according to a previous method [13] with some modifications. Dry heparin and LMWHs (100 μg in 10 μL in ultrapure water) were added to 100 μL of buffer (50 mM ammonium acetate, 2 mM, calcium chloride, pH, 7). Heparin lyase I, II and III (pH optima 7) were added to each sample and mixed completely. The mixed solutions were all put in a water bath at 37 °C overnight, followed by removing the enzymes using a 3 kDa molecule weight cut-off (MWCO) spin column in order to terminate the digestion. The heparin and LMWHs could be fully decomposed into disaccharide products, after which they were lyophilized and re-dissolved in 100 μL of ultrapure water at a concentration of 1 μg/μL.

2.5.1. Liquid chromatography-mass spectrometry (LC-MS) analysis

LC-MS analyses were conducted on an Agilent 1200 LC/MSD instrument (Agilent Technologies, Wilmington, Delaware) equipped with a Poroshell 120 C18 column (2.1 × 100 mm^2, 2.7 μm, Waters, Milford, USA), a 6300 ion trap and a binary pump followed by a UV detector equipped with a high-pressure cell. Eluent A and B were water-acetonitrile (85:15, v/v) and water-acetonitrile (35:65, v/v), respectively, containing 12 mM tributylamine and 38 mM ammonium acetate. Both eluents were adjusted to pH 6.5 with acetic acid. For disaccharide analysis, a gradient of solution A for 5 min was performed, which was followed by a linear gradient of solution B (0–40%) for 10 min at a flow rate of 150 μL/min.

2.6. FT-IR and NMR spectra

For FT-IR analysis, heparin samples were blended with KBr powder, ground for 10 min in an agate mortar and then pressed into KBr pellets. FT-IR spectra of heparin and LMWHs were collected on Nicolet 5700 spectrometer (Thermo Fisher Scientific, Waltham, USA) using the wavenumber from 4000 to 400 cm^{-1}, with resolution of 2 cm^{-1}.

For NMR analysis, the UFH and LMWH were dissolved in 500 μL deuteroxide (99.9%) and then evaporated twice through freeze drying before being dissolved again in 500 μL of deuteroxide (99.9%). The ^1H NMR spectra were recorded on a Bruker AVANCE III 800 (Bruker, Germany) at 25 °C.

2.7. Top-down analysis

The top-down analysis was executed according to a previously described method [14]. LMWH-1 and LMWH-4 were separated using a Luna HILIC column (2.0 × 150 mm^2, 200 Å, Phenomenex, Torrance, CA). Mobile phase A and B were 5 mM ammonium acetate and water-acetonitrile (2/98, v/v), respectively. The gradient was performed from 5% A to 70% A over 7 min at a flow rate of 250 μL/min, and then it was reset to 5% A. The LC column was directly connected online to the standard ESI source of LTQ-Orbitrap XL FT MS (Thermo Fisher Scientific, San-Jose, CA). All the parameters were optimized using Arixtra™ so as to decrease the insource fragmentation, sulfate loss and the noise/signal in the negative-ion mode. The optimized source parameters were as followed: spray voltage, 4.2 kV; capillary voltage, −40 V; tube lens voltage, −50 V; capillary temperature, 275 °C, sheath flow rate, 30 L/min, auxiliary gas flow rate, 6 L/min. Both the FT mass spectra were obtained at a resolution of 60,000 with 400–2000 Da mass range.

2.7.1. Bioinformatics

Charge deconvolution was conducted using DeconTools software. The structural assignments of LMWHs and the acquisition of hypothesis database were both performed on GlycReSoft 1.0 software with the parameters shown in Supporting Information (Fig. S1). All of the quantitative data was normalized to the total identified oligosaccharides peak area (%).

2.8. Anticoagulant assays

In vitro clotting assays including activated partial thromboplastin time (APTT) and thrombin time (TT) were performed using human blood donated by a volunteer without a history of thrombosis or bleeding. We collected blood in evacuated tubes with sodium citrate, followed by centrifugation at 3600 rpm for 8 min. The supernatant plasma was removed for further tests. The anticoagulant assays (APTT and TT) of unfractionated heparin, LWMHs, enoxaparin, nadroparin and parnaparin were executed using automatic processing according to the methods as described [15] on a coagulometer (RAC-120, China). The results are presented as international units/mg (IU/mg).

2.9. Inhibition of thrombin or FXa by AT in the presence of UFH and LWMHs

The inhibition experiments were performed in a 96-well micro plate as described [12] with some modifications. The reactant solutions contained AT (0.5 IU/mL) and different concentrations of samples in 40 μL of Tris/polyethylene glycol (TS/PEG) buffer. Then 40 μL of FIIa (5 IU/mL) or FXa (0.4 IU/ml) was added to trigger the reaction, followed by incubation at 37 °C for 1 min. After that, 40 μL of TS/PEG buffer including 0.625 mM colorimetric substrate of FIIa or 1 mM chromogenic substrate SXa-11 of FXa was added and the absorbance of reaction solution was recorded at 405 nm at intervals of 15 s within a period of 5 min. The change rate of absorbance was proportional to the FIIa and FXa activity remaining in the incubation mixtures. United States Pharmacopoeia (USP) heparin was selected as a control and the anti-Xa/anti-IIa was calculated using a standard curve of various concentrations of USP heparin (0.1–2 IU/mL).

2.10. Statistical analysis

Each treatment was repeated three times. All data were expressed as the mean ± standard deviation and statistically evaluated with Excel software.

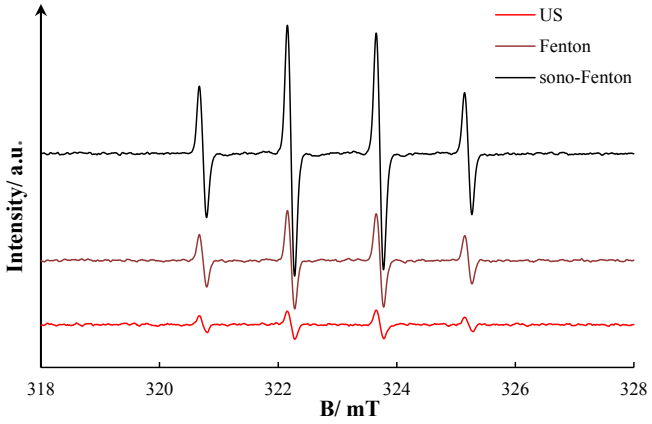

Fig. 1. Electron spin-resonance spectroscopy of different degradation systems.

3. Results and discussion

3.1. The sono-Fenton system can produce more ·OH radicals

Hydroxyl radicals (·OH) are an important reactive oxygen species with a strong electron capacity, an oxidation potential of 2.8 V, and its oxidizing power is second only to fluorine in nature [16]. Studies have shown that ·OH radicals can rapidly react with most organic compounds, attacking the groups in these organic compounds, breaking their structures and degrading these organic compounds. There were different levels of ·OH radicals content for a single ultrasound treatment, Fenton system and sono-Fenton system treatments (Fig. 1). There were four distinct signal peaks in the ESR spectra with peak intensity ratio of 1:2:2:1. The g-factor was 2.0023 and the AH and AN value were both 1.49 mT, which could demonstrate that the overall signal peak represented ·OH radicals. It was clear that the peak intensity of sono-Fenton treatment was significantly higher than that of ultrasound treatment or Fenton system alone, indicating that sono-Fenton could generate more ·OH radicals conducive to depolymerizing macromolecular. It was in accord with the previous report [17]. Therefore, we selected sono-Fenton process for preparing LMWHs.

3.2. Effect of different treatment factors on the Mw of heparin

We examined the effect of temperature, ultrasonic intensity, amount of hydrogen peroxide, the concentration of ferrous iron and pH on the degradation efficiency to investigate the optional parameters to prepare LMWHs. The sono-Fenton reaction significantly accelerated the degradation of heparin because the higher concentration of generated ·OH radicals could react with heparin by abstracting a hydrogen atom to bring about depolymerization and structural changes (Fig. 2).

3.2.1. Temperature

We explored the effect of temperature on the preparation of LMWHs since it was considered as a critical factor to regulate the reaction rate in chemical processes. The degradation efficiency significantly increased when the temperature rose from 10 to 30 °C (Fig. 2a), which was in accord with the understanding that higher temperature was likely to form more cavitation bubbles to degrade the organics during the ultrasonic process [18]. Surprisingly, there was a conspicuous decline in the degradation efficiency when the temperature continued to rise to 40 °C. The reason may be that excessively high temperature can result in the sedimentation of Fe^{2+} and self-decomposition of H_2O_2, which would reduce the efficiency of organic compound degradation and the reaction rate [19]. The increasing temperature also tends to speed up cavitation cushioning, decreasing the degradation efficiency of organics [20].

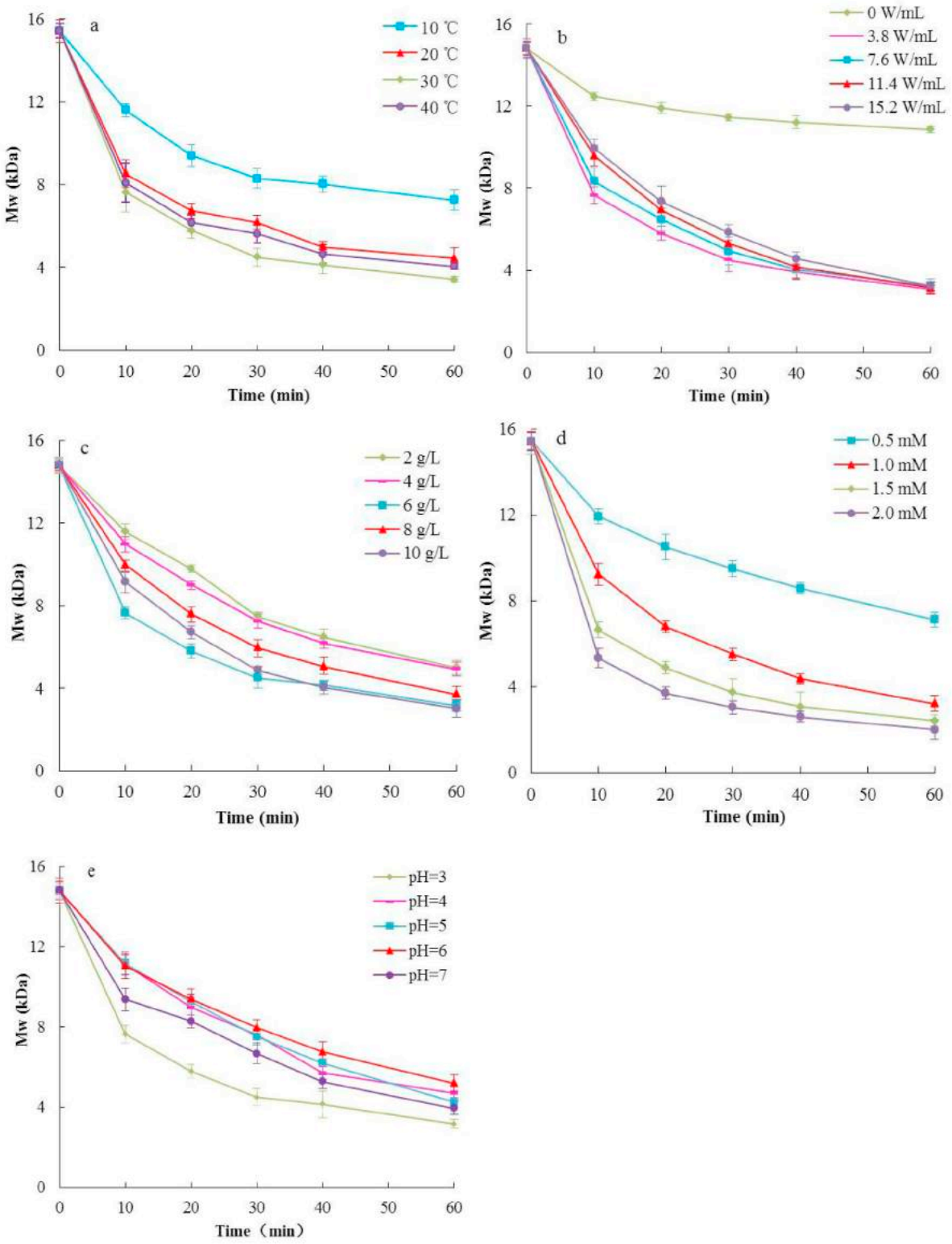

Fig. 2. Effect of different treatment factors on the Mw of heparin. a. temperature; b. ultrasonic intensity; c. H_2O_2 concentration; d. Fe^{2+} concentration; e. pH.

3.2.2. *Ultrasonic intensity*

The effect of ultrasonic intensity on degradation efficiency was investigated since it is regarded as a significant operational parameter in sono-chemical treatments to govern the formation of ·OH radicals and cavitation bubbles [21]. The results in Fig. 2b show that ultrasound further enhances the Fenton process in degrading heparin, and that ultrasonic power was not the most important parameter in heparin degradation. While ultrasound functioned to enhance the Fenton process, a low intensity of ultrasonic energy was sufficient to achieve the rapid degradation. For example, a single Fenton treatment (1.5 mM Fe^{2+} and 6 g/L H_2O_2 at 30 °C) degraded heparin from 14.8 kDa to 10.9 kDa in 60 min. In contrast, sono-Fenton treatment under the same conditions greatly accelerated the degradation process, as demonstrated by the appearance of much smaller 3.3 kDa products within

Table 2
The Mw and polydispersity index of UFH and LMWHs.

Sample	Mn (kDa)	Mw (kDa)	PI (Mw/Mn)	DP
UFH	10.03	14.81	1.48	41
LMWH-1	4.92	6.83	1.39	21
LMWH-2	3.71	4.87	1.31	16
LMWH-3	2.99	3.74	1.25	12
LMWH-4	2.03	2.43	1.19	8

60 min.

The heparin degradation efficiency declined slightly when the ultrasonic intensity was elevated from 3.8 to 15.2 W/mL. This was due to the fact that ultrasound, generating instantaneous high heat and high pressure [22], could decompose the hydrogen peroxide at the temperature of 30 °C, causing it to fail to react with Fe^{2+} to a maximum extent. This would lead to decrease the generation of ·OH radicals and, thus, limit heparin degradation efficiency. The stronger the ultrasonic intensity was, the more hydrogen peroxide was decomposed. Hence, we selected the ultrasonic power of 3.8 W/mL as the optimum reaction condition to both save energy and increase degradation efficiency.

3.2.3. Hydrogen peroxide concentration

As shown in Fig. 2c, hydrogen peroxide concentration played an important role in the degradation efficiency. Increasing H_2O_2 concentration from 2 g/L to 6 g/L (with the Fe^{2+} concentration of 1 mM) caused a clear enhancement in the efficiency of heparin degradation, but a decline in the reaction efficiency was observed when the H_2O_2 concentration was greater than 6 g/L. While increasing amount of H_2O_2 generally benefits the generation of ·OH radicals to decompose the organics [18], the slight decline of reaction observed at high H_2O_2 concentration was attributed to the consumption of ·OH through various processes including the scavenging effect of H_2O_2 and recombination of ·OH. In addition, the generation of ·OOH by the reaction between concentrated H_2O_2 and ·OH tended to reduce the degradation efficiency of heparin in sono-Fenton treatment [23] (see Eq. (2)–(4)).

$$H_2O_2 + \cdot OH \rightarrow \cdot OOH + H_2O \quad (2)$$

$$\cdot OOH + \cdot OH \rightarrow H_2\ O + O_2 \quad (3)$$

$$2 \cdot OH \rightarrow H_2O_2 \quad (4)$$

3.2.4. Concentration of ferrous iron

We also studied the effect of the concentration of ferrous iron on degradation efficiency. As shown in Fig. 2d, heparin degradation efficiency increased significantly with Fe^{2+} concentration rising from 0.5 mM to 2.0 mM with 6 g/L of H_2O_2, suggesting that more ferrous irons could contribute to producing a greater concentration of ·OH radicals under certain conditions [23]. At the beginning of sono-Fenton process, more hydroxyl radicals generated by Fenton reagent attacked the sugar chain because of sufficient H_2O_2 concentration from 0 to 40 min. Nevertheless, there was a slight difference in the Mw of LMWHs between 1.5 and 2 mM after 60 min and the degradation rate slowed down because of the consumption of H_2O_2. Hence, the Fe^{2+} concentration of 1.5 mM was selected as the optimal concentration.

3.2.5. Initial pH

Initial pH is a vital parameter for the degradation of organic compounds by sono-Fenton process, so the influence of pH on the reaction efficiency was also investigated. The degradation efficiency of heparin negatively correlated with pH through a range of value from 3 to 6, while it increased at initial pH of 7 (Fig. 2e). At pH of 3, the formation of hydroxyl radicals produced by decomposition of hydrogen peroxide was favored, thereby improving the availability of free radicals to accelerate heparin oxidation. At pH ≥ 4, the precipitation of $Fe(OH)_2$ impacted the reduction of Fe^{2+} to Fe^{3+}, decreasing the regeneration of ·OH radicals and reducing degradation efficiency [23]. At pH of 7, a small amount of nano-scale $Fe(OH)_3$ precipitates formed in the solution, changing the reaction system from a homogeneous to a heterogeneous system. Ultrasound processing generates electronic transitions on the surface of the $Fe(OH)_3$ particles, creating ·OH radicals to enhance the redox reaction [24]. Therefore, we concluded that the optimum pH value for the high-efficiency degradation of heparin was pH of 3.

Sono-Fenton treatment resulted in a rapid degradation of heparin, which was ascribed to the generation of ·OH radicals that could react with the heparin polysaccharide and bring about hydrogen atom abstraction and chain breakage. The temperature, Fenton reagent concentration, and pH all impacted the degradation of heparin, which was evidenced by a greatly reduced molecular weight with a degradation rate that was similar at different ultrasound intensities.

3.3. Disaccharide compositional analysis of UFH and LMWHs

By controlling the duration of treatment, the optimized sono-Fenton system afforded four forms of degraded heparin having distinct molecular weights, polydispersity index (PI) and degree of polymerization (DP) (Table 2). The products with 0, 10, 20, 30, and 60 min were defined as UFH, LMWH-1, LMWH-2, LMWH-3 and LMWH-4, respectively.

Disaccharide analysis is the basis for exploring the fine structure and is required to establish a structure-activity relationship for heparin glycosaminoglycans [25]. Unfractionated heparin contained 7 major disaccharide units, the content of which ranging from high to low was ΔUA2S-GlcNS6S (where ΔUA represents deoxy-α-L-threo-hex-4-enopyranosyluronic acid, GlcN represents *N*-acetylglucosamine and S represents sulfo group) > ΔUA-GlcNS6S > ΔUA2S-GlcNS > ΔUA-GlcNAc6S > ΔUA2S-GlcNAc6S > ΔUA-GlcNS > ΔUA-GlcNAc, and ΔUA2S-GlcNAc component was not detected (Fig. 3). The percentage of disaccharide components of LMWHs varied with sono-Fenton treatment time. Under prolonged sono-Fenton treatment, a new disaccharide composition ΔUA2S-GlcNAc was formed presumably due to the 6-*O*-desulfation of ΔUA2S-GlcNAc6S. There was also a slight increase in ΔUA2S-GlcNAc content in LMWHs, resulting from the loss of sulfo groups in ΔUA-GlcNAc6S and ΔUA2S-GlcNAc6S. In addition, ΔUA2S-GlcNS6S content significantly increased, having the highest proportion (80.12%) in LWMH-4. However, the contents of other disaccharide constituents, such as ΔUA-GlcNS, ΔUA-GlcNS6S and ΔUA2S-GlcNS, were reduced over time. Among these disaccharide components, the greatest change was in ΔUA-GlcNS6S (Fig. 3), which might be due to the assumption that the produced ·OH radicals in the sono-Fenton system were more likely to selectively attack certain sites within heparin.

3.4. Structural characteristics of UFH and LMWHs by FT-IR

FT-IR is a powerful method for the gross characterization of the carbohydrates [26]. The major absorption peak at around 3432 cm^{-1} was assigned to the stretching vibration of hydroxyl groups and this peak was broadened by the intramolecular hydrogen bond formed by O—H (Fig. 4). The absorption at around 2938 cm^{-1} was assigned to C—H stretching of CH_2 groups. These two major absorption peaks were commonly observed for polysaccharides [27]. Two characteristic absorption bands at 1231 cm^{-1} and 809 cm^{-1} could be clearly observed, corresponding to the asymmetrical S=O stretching vibration of $O—SO_3^-$ and the symmetrical C—O—S vibration of $C—O—SO_3$ group, respectively [28]. In general, all samples had similar infrared absorption properties and sono-Fenton reaction did not remarkably alter the characteristics of heparin. Some minor structural changes could be observed by FT-IR. Compared with UFH, both their intensities were slightly reduced after treatment, indicating that hydroxyl radicals tended to result in some sulfo group loss. Comparison of before and after degradation of UFH suggested that the intensity of the featured

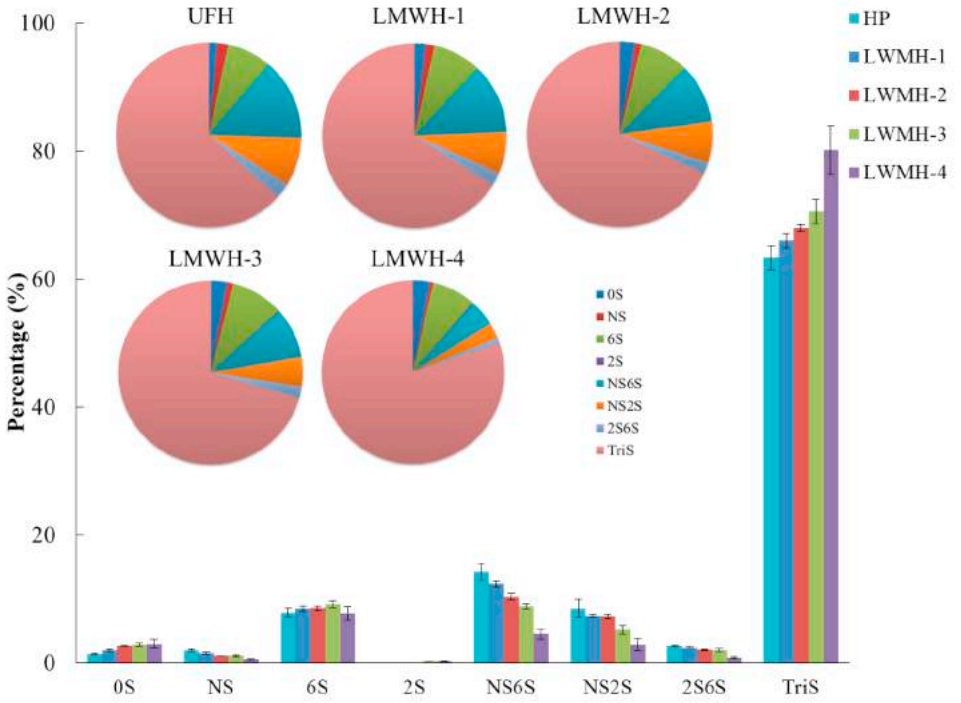

Fig. 3. Disaccharide components of heparin and LMWHs by US-Fenton process with different time. 0S, ΔUA-GlcNAc; NS, ΔUA-GlcNS; 6S, ΔUA-GlcNAc6S; 2S, ΔUA2S-GlcNAc; NS6S, ΔUA-GlcNS6S; NS2S, ΔUA2S-GlcNS; 2S6S, ΔUA2S-GlcNAc6S; TriS, ΔUA2S-GlcNS(6S).

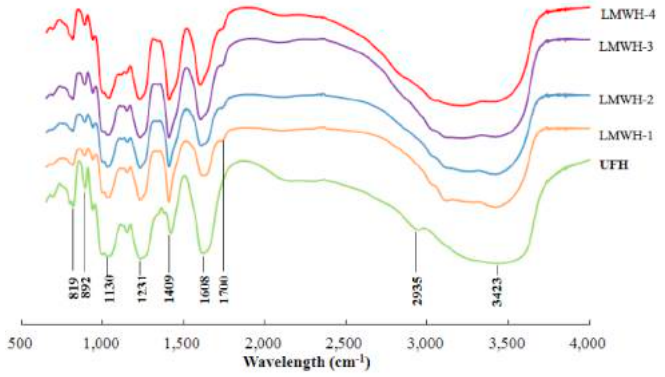

Fig. 4. FT-IR spectra of heparin and LMWHs.

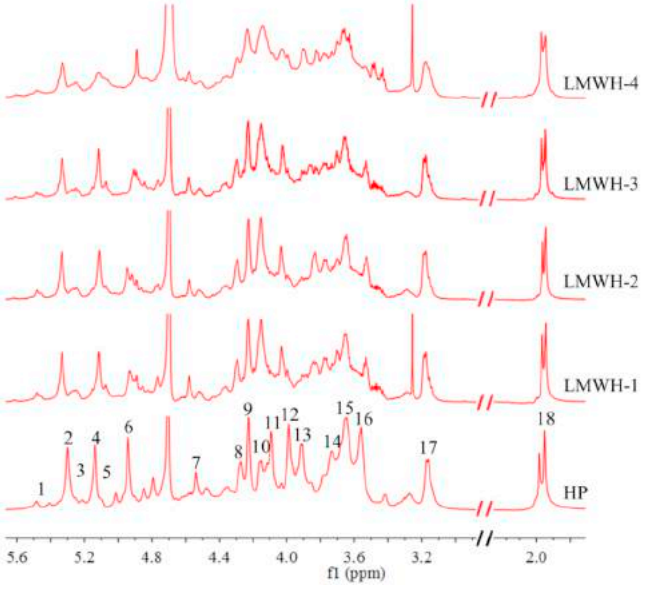

Fig. 5. ^{1}H NMR spectra of heparin and LMWHs. 1: GlcNS3S6S H_1; 2: GlcNS6S H_1; 3: GlcNS H_1 linked to IdoA2S; 4: IdoA2S H_1; 5: IdoA H_1; 6: IdoA2S H_5 linked to GlcNS6S; 7: GlcA H_1; 8: GlcNS6S H_{6a}; 9: IdoA2S H_2; 10: GlcNS6S H_{6b}; 11: IdoA2S H_3; 12: IdoA2S H_4; 13: GlcNS6S H_5; 14: GlcNS H_6; 15: GlcNS6S H_4; 16: GlcNS H_3, GlcNS6S H_3; 17: GlcNS6S H_2; 18: N-$COCH_3$, GlcNAc.

absorption at 1608 cm^{-1} assigned to the bending vibration of amido groups (−NH_2) decreased while that at 1409 cm^{-1} corresponding to the symmetric stretching of the nitroso-group (−NO_2) increased, which demonstrated that the amino groups of heparin might be oxidized to nitroso-group by ·OH radicals. In addition, the absorption peak at 1130 cm^{-1} (C—O stretching) decreased and a new absorption band of C═O stretching at 1700 cm^{-1} increased by oxidation reaction, indicating that the C—O group might be oxidized to carbonyl groups by the ·OH radicals [29].

3.5. NMR spectra of UFH and LMWHs

^{1}H NMR spectroscopy is commonly used to identify the structural characterization of viscous glycosaminoglycans. The proton spectra of LMWHs were similar to those of UFH, suggesting that sono-Fenton treatment did not change the fundamental structure of heparin (Fig. 5). Compared with UFH, there were more signal peaks in the degraded LMWHs at prolonged treatment times because of the decrease of molecular weight and the weakening of the interaction force between the sugar rings. The signal peaks at 5.48 ppm, 5.33 ppm, 5.11 ppm, 5.08 ppm and 4.58 ppm corresponded to the anomeric hydrogen signals of GlcNS3S6S, GlcNS6S, IdoA2S, IdoA, and GlcA, respectively. The peak at 5.26 ppm was assigned to the anomeric hydrogen on GlcNS connected to IdoA2S. Moreover, the peaks at 4.23 ppm, 4.10 ppm, 4.01 ppm, and 4.93 ppm were assigned to H-2, H-3, H-4, and H-5 on IdoA2S, respectively. It can be seen from the anomeric hydrogen region that there were almost no obvious changes in the anomeric hydrogen signal corresponding to each sugar ring since ·OH radicals did not

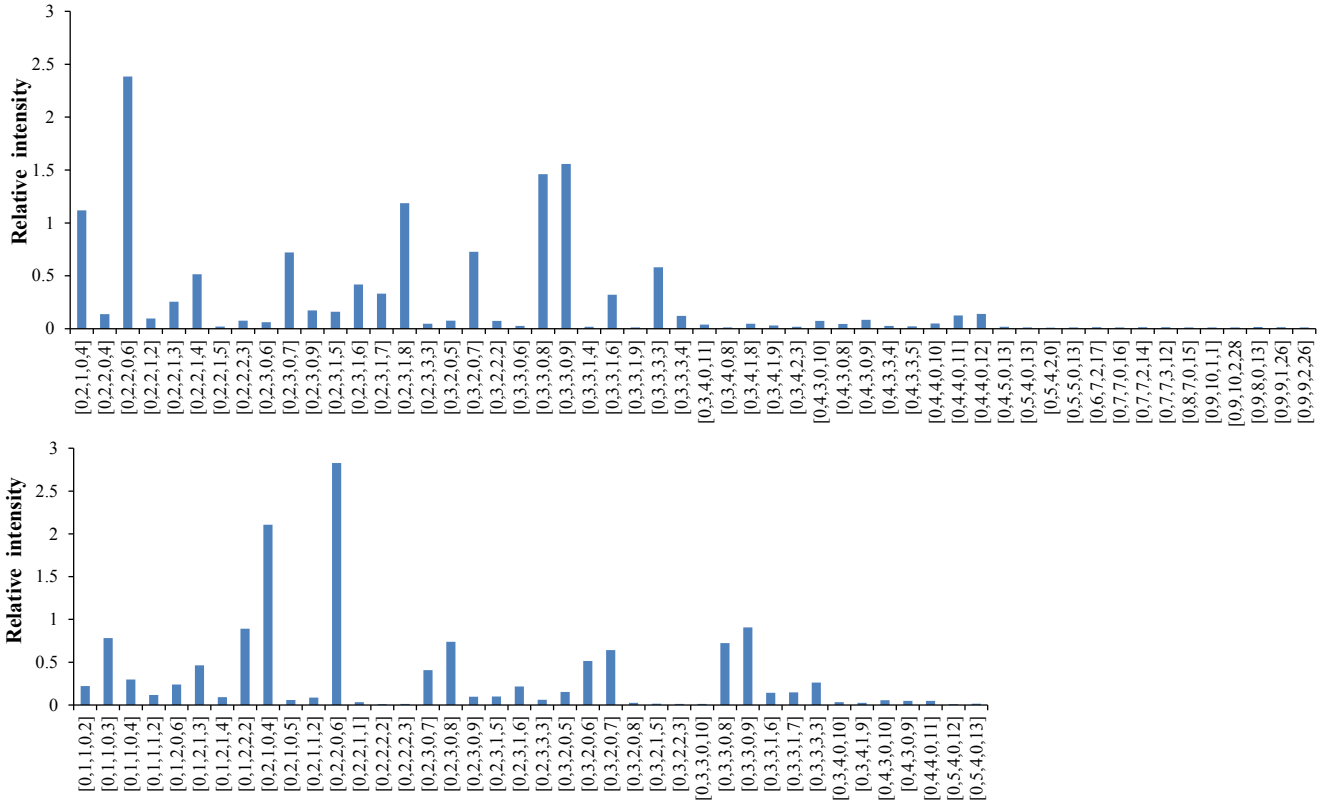

Fig. 6. Top-down approach using HILIC LC–FT–ESI–MS to characterize LMWH-1 and LMWH-4. (a) Detected LMWH-1 oligosaccharides. (b) Detected LMWH-4 oligosaccharides. The oligosaccharides are labeled with the number of [HexA, HexA, GlcN, Ac, SO_3] moieties present in each structure.

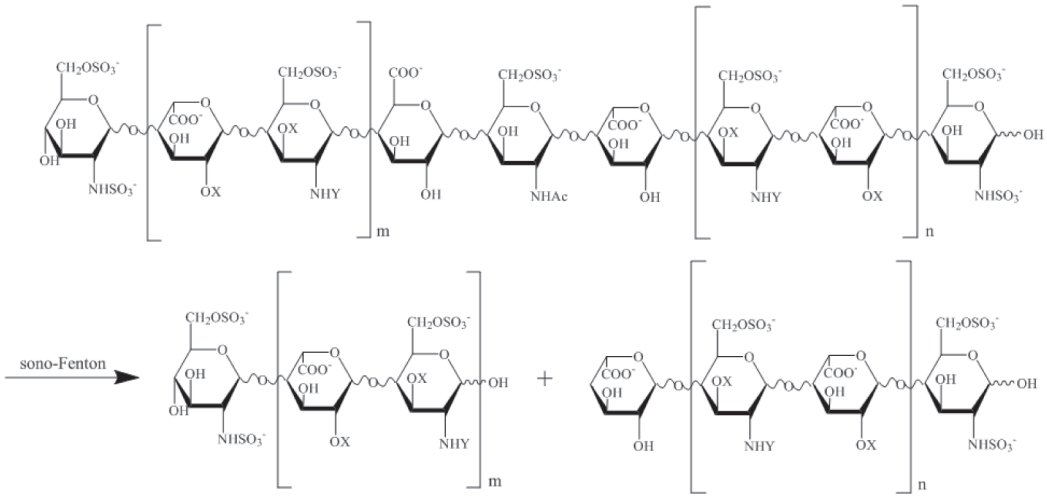

Fig. 7. Depolymerization of heparin to prepare LWMH.

change the overall structure of heparin. This conclusion could be supported by the observation that the disaccharide analysis showed just a few differences in the contents of the disaccharide components corresponding to a variation in peak area. We next conducted a top-down analysis to further study on the degradation mechanism of heparin and the acting sites.

3.6. Top-down analysis of LMWH-1 and LMWH-4

The relative abundance of oligosaccharide components corresponds to LMWH-1 and LMWH-4 (Table S1). We excluded fractions with a relative abundance below 0.01 and the results are presented in Fig. 6. More oligosaccharide information was obtained for LMWH-1 than for LMWH-4 as LMWH-1 was degraded by sono-Fenton for a shorter time. In addition, the information on oligosaccharide fractions with larger Mw was acquired, such as [0, 9, 9, 2, 26], [0, 9, 10, 1, 1] and [0, 9, 10, 2, 28]. The Mw of LMWH-4 was greatly reduced because of the longer reaction time and, thus, oligosaccharide components were mainly concentrated within 9 sugar residues. Among the compositions of LMWH-1 and LMWH-4, the content of fractions, including [0, 1, 2, 0,

Table 3
APTT, TT, anti-Xa and anti-IIa activities of unfractionated heparin (UFH), commercial LMWHs and LMWHs produced by US-Fenton system.

Sample	APTT* IU/mg	TT* IU/mg	Anti-FXa, IU/mg	Anti-FIIa, IU/mg	Anti-FXa/Anti-FIIa
UFP	135	135	135	135	1
LMWH-1	64.81 ± 1.31	54.14 ± 2.97	124.11 ± 3.21	81.42 ± 4.22	1.52
LMWH-2	29.87 ± 2.06	< 46.42	117.83 ± 4.17	44.76 ± 2.75	2.63
LMWH-3	16.69 ± 0.14	< 46.42	81.85 ± 2.84	41.73 ± 1.59	1.96
LMWH-4	< 7.58	< 46.42	48.98 ± 2.17	37.33 ± 3.52	1.31
Parnaparin	27.64 ± 5.35	< 46.42	106.64 ± 5.23	46.71 ± 2.94	2.28
Enoxaparin	29.21 ± 3.00	< 46.42	138.03 ± 8.16	39.31 ± 2.33	3.51
Nadroparin	30.58 ± 4.51	< 46.42	130.66 ± 1.39	50.33 ± 1.48	2.59

n = 3.
* The activities of agents to prolong APTT, PT, and TT are expressed by the concentration of each agent (IU/mg) that is required to double the APTT, PT, or TT.

4], [0, 2, 2, 0, 6], [0, 3, 2, 0, 7], [0, 3, 3, 0, 8] and [0, 3, 3, 0, 9], was higher than others, indicating that the degradation products had a certain degree of consistency and there was a certain regularity about oxidative degradation. The isomers could not be distinguished in this quantitative analysis, but from the statistics of the data set, the ratio of [0, a, a + 1, b, c] was higher than that of [0, a + 1, a, d, e], where 'a' was a positive integer. This suggested that degradation products of UFH were dominated by hexosamine (HexN) at the end group, which might result from hexuronic acid (HexA) being more susceptible to attack by · OH radicals. Similar results have been reported by others [12]. Fig. 7A suggests a feasible sono-Fenton mechanism for the generation of LWMHs, wherein X represents H or SO_3^- group and m and n stands for the number of repeating units.

3.7. Anticoagulant activity

Following structural analysis, the anticoagulant activities of UFH, LMWHs and commercial products were determined using APTT and TT of plasma clotting assays (Table 3). These were used to determine the blood clotting inhibitory activity of anticoagulants through the intrinsic and common pathways of the coagulation cascade, respectively. Notably, the results of both APTT and TT assays indicated that the anticoagulant activity of these heparins was significantly influenced by Mw and UFH, and LMWHs displayed different anticoagulant mechanism. Specifically, UFH showed the APTT of 135 IU/mg, much lower than that of LMMHs including commercial LMWHs. In comparison, the APTT of LMWH-1, LMWH-2 and LMWH-3 were decreased to 64.81 IU/mg, 29.87 IU/mg and 16.69 IU/mg, respectively, while LMWH-4 exhibited negligible effect on both APTT and TT, suggesting that UFH exhibited anticoagulant activity by acting on both intrinsic and common pathways while LMWHs mainly by intrinsic pathways.

Anticoagulant activity was also determined using purified blood coagulation factor assays. The results showed that the inhibitory effects of thrombin (FIIa) and FXa mediated by AT were significantly reduced with decreasing molecular weight. However, the anti-FXa activity of all depolymerized LMWHs was much higher than anti-FIIa activity, resulting in increased anti-FXa/anti-FIIa ratio than that of unfractionated heparin and, hence, reduced side effects [30]. Notably, the anti-FXa and anti-FIIa activities of LMWH-2 were 117.83 IU/mg (± 4.17) and 44.76 IU/mg (± 2.75), respectively, with the largest anti-FXa/anti-FIIa ratio of 2.63 among all the LMWHs produced by sono-Fenton system. This ratio was similar to that of commercial Nadroparin (2.59), suggesting Mw control was important to anticoagulant activity and adverse effects. Thus, sono-Fenton system might be used for fast preparation of LMWHs with relatively high anticoagulant activity and reducing side effects. Also, 87% of the anti-FXa of LMWH-2 was retained compared to UFH (135 IU/mg) starting material, indicating that sono-Fenton system largely preserved the AT pentasaccharide binding sequence.

4. Conclusions

In the current study, we investigated a highly-efficient approach to prepare LMWHs with anticoagulant properties comparable to commercial products. In our method, we combined ultrasonic wave and Fenton system, which was much more effective than any single treatment. We also identified the relatively high-efficiency parameters to prepare LMWHs by screening out the best conditions of temperature, ultrasonic intensity, H_2O_2 concentration, Fe^{2+} concentration and pH. Disaccharide composition, FT-IR, NMR and top-down analysis were applied to determine the composition and preliminary structural features of LMWHs. Our results demonstrated that the sono-Fenton system degraded heparin to generate LWMHs, which possessed elevated anticoagulant activity and were dominated by HexN at the end group, and that HexA was more likely to be damaged by hydroxyl radicals. In summary, we suggest the sono-Fenton system as an efficient approach to prepare the LMWHs.

In the future, we plan to optimize the parameters using statistical experimental design to further evaluate these factors and find the optimal conditions, which is much more effective than "one factor at a time" approach. In addition, further investigation is needed into the surprising lack of a positive correlation of degradation rate and ultrasonic power.

Acknowledgements

This work was supported by National Science Foundation of China (31301417) and the U.S. National Institutes of Health (HL094463).

Appendix A. Supplementary data

Supplementary data to this article can be found online at https://doi.org/10.1016/j.ultsonch.2018.11.016.

References

[1] D. Wardrop, D. Keeling, The story of the discovery of heparin and warfarin, Br. J. Haematol. 6 (2008) 757–763.
[2] A. Köwitsch, G. Zhou, T. Groth, Medical application of glycosaminoglycans: a review, J. Tissue Eng. Regener. Med. 1 (2018) e23–e41.
[3] R. Sasisekharan, G. Venkataraman, Heparin and heparan sulfate: biosynthesis, structure and function, Curr. Opin. Chem. Biol. 6 (2000) 626–631.
[4] J. Hirsh, R. Raschke, Heparin and Low-Molecular-Weight Heparin, Chest 3 (2004) 188S–203S.
[5] D. Lee, B.H. Kim, S. Kim, J. Kim, H. Lee, S. Jung, Preparation of low molecular weight heparin by microwave discharge electrodeless lamp/TiO_2 photo-catalytic reaction, J. Nanosci. Nanotechnol. 1 (2015) 680–683.
[6] B. Cosmi, G. Palareti, Old and new heparins, Thromb. Res. 129 (2012) 388–391.
[7] X. Ma, L. Zhang, W. Wang, M. Zou, T. Ding, X. Ye, D. Liu, Synergistic effect and mechanisms of combining ultrasound and pectinase on pectin hydrolysis, Food Bioprocess Technol. 7 (2016) 1249–1257.
[8] L. Zhang, X. Zhang, D. Liu, T. Ding, X. Ye, Effect of degradation methods on the structural properties of citrus pectin, LWT – Food Sci. Technol. 2 (2015) 630–637.
[9] O. Achour, N. Bridiau, A. Godhbani, F. Le Joubioux, S. Bordenave Juchereau, F. Sannier, J. Piot, I. Fruitier Arnaudin, T. Maugard, Ultrasonic-assisted preparation of a low molecular weight heparin (LMWH) with anticoagulant activity, Carbohydr.

Polym. 2 (2013) 684–689.
[10] X. Ma, W. Wang, D. Wang, T. Ding, X. Ye, D. Liu, Degradation kinetics and structural characteristics of pectin under simultaneous sonochemical-enzymatic functions, Carbohydr. Polym. (2016) 176–185.
[11] Z. Zhi, J. Chen, S. Li, W. Wang, R. Huang, D. Liu, T. Ding, R.J. Linhardt, S. Chen, X. Ye, Fast preparation of RG-I enriched ultra-low molecular weight pectin by an ultrasound accelerated Fenton process, Sci. Rep.-Uk 1 (2017).
[12] J. Li, S. Li, Z. Zhi, L. Yan, X. Ye, T. Ding, L. Yan, R. Linhardt, S. Chen, Depolymerization of fucosylated chondroitin sulfate with a modified Fenton-system and anticoagulant activity of the resulting fragments, Mar. Drugs 9 (2016) 170.
[13] L. Lin, X. Liu, F. Zhang, L. Chi, I.J. Amster, F.E. Leach, Q. Xia, R.J. Linhardt, Analysis of heparin oligosaccharides by capillary electrophoresis–negative-ion electrospray ionization mass spectrometry, Anal. Bioanal. Chem. 2 (2017) 411–420.
[14] X. Wang, X. Liu, L. Li, F. Zhang, M. Hu, F. Ren, L. Chi, R.J. Linhardt, GlycCompSoft: software for automated comparison of low molecular weight heparins using top-down LC/MS data, PLoS One 12 (2016) e167727.
[15] S. Ouerghemmi, S. Dimassi, N. Tabary, L. Leclercq, S. Degoutin, F. Chai, C. Pierlot, F. Cazaux, A. Ung, J. Staelens, N. Blanchemain, B. Martel, Synthesis and characterization of polyampholytic aryl-sulfonated chitosans and their in vitro anticoagulant activity, Carbohydr. Polym. (2018) 8–17.
[16] A.R. Ribeiro, O.C. Nunes, M.F.R. Pereira, A.M.T. Silva, An overview on the advanced oxidation processes applied for the treatment of water pollutants defined in the recently launched Directive 2013/39/EU, Environ. Int. (2015) 33–51.
[17] C. Gong, J. Jiang, D.A. Li, S. Tian, Ultrasonic application to boost hydroxyl radical formation during Fenton oxidation and release organic matter from sludge, Sci. Rep.-Uk. (2015) 11419.
[18] N. Golash, P.R. Gogate, Degradation of dichlorvos containing wastewaters using sonochemical reactors, Ultrason. Sonochem. 5 (2012) 1051–1060.
[19] J. Farias, E.D. Albizzati, O.M. Alfano, Kinetic study of the photo-Fenton degradation of formic acid, Catal. Today. 1–2 (2009) 117–123.
[20] C. Wang, Y. Shih, Degradation and detoxification of diazinon by sono-Fenton and sono-Fenton-like processes, Sep. Purif. Technol. (2015) 6–12.
[21] C. Wang, Z. Liu, Degradation of alachlor using an enhanced sono-Fenton process with efficient Fenton's reagent dosages, J. Environ. Sci. Health., Part B 7 (2015) 504–513.
[22] W. Wang, W. Chen, M. Zou, R. Lv, D. Wang, F. Hou, H. Feng, X. Ma, J. Zhong, T. Ding, X. Ye, D. Liu, Applications of power ultrasound in oriented modification and degradation of pectin: a review, J. Food Eng. 98–107 (2018).
[23] G. Harichandran, S. Prasad, SonoFenton degradation of an azo dye, Direct Red, Ultrason. Sonochem. (2016) 178–185.
[24] A.D. Bokare, W. Choi, Review of iron-free Fenton-like systems for activating H_2O_2 in advanced oxidation processes, J. Hazard. Mater. (2014) 121–135.
[25] Y. Chang, B. Yang, X. Zhao, R.J. Linhardt, Analysis of glycosaminoglycan-derived disaccharides by capillary electrophoresis using laser-induced fluorescence detection, Anal. Biochem. 1 (2012) 91–98.
[26] P. Li, J. Xia, Z. Nie, Y. Shan, Pectic oligosaccharides hydrolyzed from orange peel by fungal multi-enzyme complexes and their prebiotic and antibacterial potentials, LWT – Food Sci. Technol. (2016) 203–210.
[27] L. Zhang, X. Ye, T. Ding, X. Sun, Y. Xu, D. Liu, Ultrasound effects on the degradation kinetics, structure and rheological properties of apple pectin, Ultrason. Sonochem. 1 (2013) 222–231.
[28] B.W. Jo, S. Choi, Degradation of fucoidans from *Sargassum fulvellum* and their biological activities, Carbohydr. Polym. (2014) 822–829.
[29] E. Vismara, M. Pierini, G. Mascellani, L. Liverani, M. Lima, M. Guerrini, G. Torri, Low-molecular-weight heparin from Cu^{2+} and Fe^{2+} Fenton type depolymerisation processes, Thromb. Haemost. 3 (2010) 613–622.
[30] Y. Buyue, J.P. Sheehan, Fucosylated chondroitin sulfate inhibits plasma thrombin generation via targeting of the factor IXa heparin-binding exosite, Blood 14 (2009) 3092–3100.